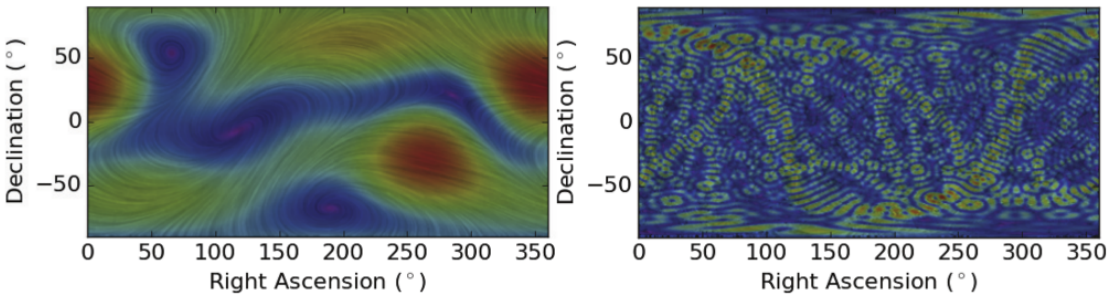

Figure 1.10: All-sky stream plots. Streamlines indicate the vector field direction, and the colours indicate the vector amplitude, from violet (zero) to red (maximum). (left) Randomly generated gravitational wave stream plot. (right) Randomly generated baryon acoustic oscillation streamlines (Darling et al. 2018b). ©AAS. Reproduced with permission.

close merging images of suitable gravitational lenses are of order hours to days, a cadence of hours may be needed to fully exploit this science case in the future. In the case of water megamasers and precision astrometric measurements, high cadence at higher radio frequencies is needed due to the frequency of the water line (even for high redshift sources, see below) and the need to have both precise measurements of the source positions and to determine any core-shift. Therefore, having a continuously operational VLBI facility, with the required frequency coverage between 1 to 22 GHz on all elements of the array, will be needed to enable studies of cosmology with variable radio sources in the future.

- **Frequency coverage:** As discussed above, using water megamaser galaxies at high redshift to probe cosmology will require a VLBI array that has continuous frequency coverage from around 10 to 22 GHz, corresponding to water megamaser galaxies within the local volume to redshift 1.2. Currently, the EVN does not have this frequency flexibility and the recent development of broad band receivers (e.g. BRAND) can provide this up to around 15 GHz, which would be sensitive to water megamaser galaxies at redshift > 0.48. Also, not all EVN antennas are equipped with 22.2 GHz receiver systems, mainly due to the surface accuracy of those antennas. By increasing the number of antennas in the array that operate at 22 GHz, the overall sensitivity to water megamaser systems in the local Universe will be improved (this is the limiting factor in current studies). Also, to measure the core-shift in radio sources so that their positions can be precisely measured requires simultaneous multi-frequency imaging, for example with a BRAND-like system.

- **Angular resolution:** Observing radio sources at higher redshift, such as in the cases of water megamaser galaxies, has the advantage of better probing the dark energy equation-of-state and also limiting the systematics associated with peculiar motions of the target source. However, observing at higher redshift also results in a smaller physical scale being observed. For example, in the case of UGC 3789 at 49.9 ± 7 Mpc, the accretion disk is about 2 mas in diameter, which is equivalent to around 0.5 pc (i.e. about 20 synthesised beams). For the same galaxy at redshifts 0.5 and 1, the angular-scale changes by a factor of between 25 and 35, meaning that the water megamaser components will no longer be resolved (disk sizes of about 0.06 to 0.08 mas). However, the larger volume of the Universe that is probed will

likely find systems that are associated with more massive black holes, which may also result in supporting larger accretion disks. In these cases, an increase in the black hole mass by two orders of magnitude would also increase the accretion disk size in a similar way. Such systems would be resolvable with a global VLBI array operating between 10 and 22 GHz. For lower mass black holes, space-based VLBI would be needed to achieve the required angular resolutions. Alternatively, there may be a few special cases at very high redshift where the water megamasers are also gravitationally lensed. In such cases, the lensing magnification may help overcome the lower angular-scales at such large distances, but would also provide two routes to constraining cosmology, one via the lensing time-delay and the other via the water megamaser geometric distances.

REFERENCES

Abbott, B. P. et al., 2017, *Nature*, **551**, 85
Banik, U. et al., 2019, *MNRAS*, **483**, 1558
Barvainis, R., Antonucci, R., 2005, *ApJ*, **628**, L89
Biggs, A. D. et al., 1999, *MNRAS*, **304**, 349
Biggs, A. D. et al., 2003, *MNRAS*, **338**, 1084
Biggs, A. D. et al., 2004, *MNRAS*, **350**, 949
Bonvin, V. et al., 2017, *MNRAS*, **465**, 4914
Bonvin, V. et al., 2018, *A&A*, **616**, A183
Braatz, J. A. et al., 2010, *ApJ*, **718**, 657
Braatz, J. A. et al., 2010, *Proc. IAUS*, **336**, 86
Bradač, M. et al., 2002, *A&A*, **388**, 373
Browne, I. W. A. et al., 2003, *MNRAS*, **341**, 13
Darling, J. et al., 2018a, *ASP Conf. Ser.*, **517**, 813
Darling, J. et al., 2018b, *ApJ*, **861**, 113
Despali, G., & Vegetti S., 2017, *MNRAS*, **469**, 1997
Despali, G. et al., 2018, *MNRAS*, **475**, 5424
Fassnacht, C. D. et al., 2002, *ApJ*, **581**, 823
Frenk, C. S., & White, S. D. M., 2012, *AnP*, **524**, 507
Gwinn, C. R. et al., 1997, *ApJ*, **485**, 87
Hartley, P. et al., 2019, *MNRAS*, **485**, 3009
Hall, A., 2019, *MNRAS*, **486**, 145
Herrnstein, J. R. et al., 1999, *Nature*, **400**, 539
Hildebrandt, H. et al., 2017, *MNRAS*, **465**, 1454
Hinshaw, G. et al., 2009, *ApJS*, **180**, 225
Hotokezaka, K. et al., 2019, *Nature Astronomy*, **2**, 1454
Hsueh, J.-W. et al., 2016, *MNRAS*, **463**, L51
Hsueh, J.-W. et al., 2017, *MNRAS*, **469**, 3713
Hsueh, J.-W. et al., 2018, *MNRAS*, **475**, 2438
Impellizzeri, C. M. V. et al., 2008, *Nature*, **456**, 927
Koopmans, L. V. E. et al., 2009, *ApJ*, **703**, L51
Lo, K. Y. et al., *ARA&A*, **43**, 625
Lovell, M. R. et al., 2012, *MNRAS*, **420**, 2318
Mao, S. et al., 2001, *MNRAS*, **323**, 301
Mao, S. A. et al., 2017, *Nature Astronomy*, **1**, 621

Massey, R. et al., 2008, *Nature*, **445**, 286
McKean, J. P. et al., 2004, *MNRAS*, **350**, 167
McKean, J. P. et al., 2007, *MNRAS*, **377**, 430
McKean, J. P. et al., 2011, *MNRAS*, **410**, 2506
McKean, J. P. et al., 2015, *PoS*, **AASKA14**, A84
Mittal, R. et al., 2007, *A&A*, **465**, 405
Miyoshi, M., et al., 1995, *Nature*, **373**, 127
MacLeod, C. L. et al., 2013, *ApJ*, **773**, 35
Mooley, K. P. et al., 2018, *Nature*, **561**, 355
Moore, B. et al., 1999, *ApJ*, **524**, L19
More, A. et al., 2009, *MNRAS*, **394**, 174
Myers, S. T. et al., 2003, *MNRAS*, **341**, 1
Peck, A. B., et al., 2003, *ApJ*, **590**, 149
Penzias, A. A., Wilson, R. W., 1965, *ApJ*, **142**, 419
Percival, W. J et al., 2010, *MNRAS*, **401**, 2148
Pesce, D. W. et al., 2018, *ApJ*, **863**, 149
Phillips, P. M. et al., 2000, *MNRAS*, **319**, L7
Planck Collaboration, 2019, *A&A*, submitted [arXiv:1807.06209]
Quinn, J. et al., 2016, *MNRAS*, **459**, 2394
Refsdal, S., 1964, *MNRAS*, **128**, 307
Reid, M. J. et al., 2013, *ApJ*, **767**, 154
Riess, A. G. et al., 1998, *AJ*, **116**, 1009
Riess, A. G. et al., 2004, *ApJ*, **607**, 665
Riess, A. G. et al., 2018, *ApJ*, **861**, 126
Schutz, B. F., 1986, *Nature*, **323**, 310
Spingola, C. et al., 2018, *MNRAS*, **478**, 4816
Spingola, C. et al., 2019a, *MNRAS*, **483**, 2125
Spingola, C. et al., 2019b, *A&A*, **630**, A108
Spiniello, C. et al., 2012, *ApJ*, **753**, L32
Suyu, S. H. et al., 2012, *ApJ*, **750**, 10
Vegetti, S. et al., 2012, *Nature*, **481**, 341
Winn, J. N. et al., 2000, *AJ*, **120**, 2868
Winn, J. N. et al., 2003, *ApJ*, **587**, 80
Winn, J. N. et al., 2004, *Nature*, **427**, 613
Wucknitz, O. et al., 2004, *MNRAS*, **349**, 14
Zhang, M. et al., 2007, *MNRAS*, **377**, 1623

2. Galaxy formation and evolution

2.1 Star-formation, accretion and feedback over cosmic time

2.1.1 Galaxy formation

One of the most important questions regarding the evolution of our Universe is how the rate of star-formation has changed throughout cosmic time – from which the history of the assembly of galaxies can be derived. Star-formation rates within individual galaxies can be traced over a large range of wavelengths in both continuum - for example ultra-violet and infrared wavelengths, and line emission such as Hα. However, in the cases of many of these tracers, the dust obscuration which is so prevalent in the most massive star-forming galaxies often results in reduced estimates of the star-formation rate, which then require significant correction terms. In addition, at high redshifts line tracers such as Hα, are transformed to parts of the electromagnetic spectrum that are not easily observed with ground-based telescopes. A recent excellent derivation of the evolution of cosmic star-formation rate density with time from Madau & Dickinson (2014), incorporating our best obscuration correction terms is shown in Figure 2.1 (left & centre).

There is a continued debate regarding both the dust obscuration in high redshift galaxies and derived corrections applied to observed ultraviolet UV emission at redshifts above 2, in addition to the contribution to the star-formation rate in the infrared (IR) from low luminosity star-forming objects (e.g. Katsianis et al., 2017). The resulting slope of the star-formation rate density (SFRD) distribution at high redshift, which is dominated by rest-frame UV data, appears somewhat flatter than that derived from IR data at redshifts above the peak of the distribution which lies close to z=2. In addition, the extinction-corrected optical/UV SFRD compilation by Hopkins & Beacom (2006), and SFRD estimates derived from high-redshift γ-ray bursts (GRBs) by Kistler et al. (2009) both suggest that the slope of the SFRD distribution above z$\sim$2 may be flatter still. This range of possible SFRD distributions is illustrated in Figure 2.1 (Right) which is taken from Gruppioni et al. (2017).

Both thermal and non-thermal radio emission can be related to the ongoing star-formation rate in galaxies at all redshifts and uniquely offers an un-obscured tracer of the current star-formation. This relationship is underlined by the observed correlation over 4 orders of magnitude in luminosity

Chapter image credit: Stephan's Quintet – HUBBLESITE.org.

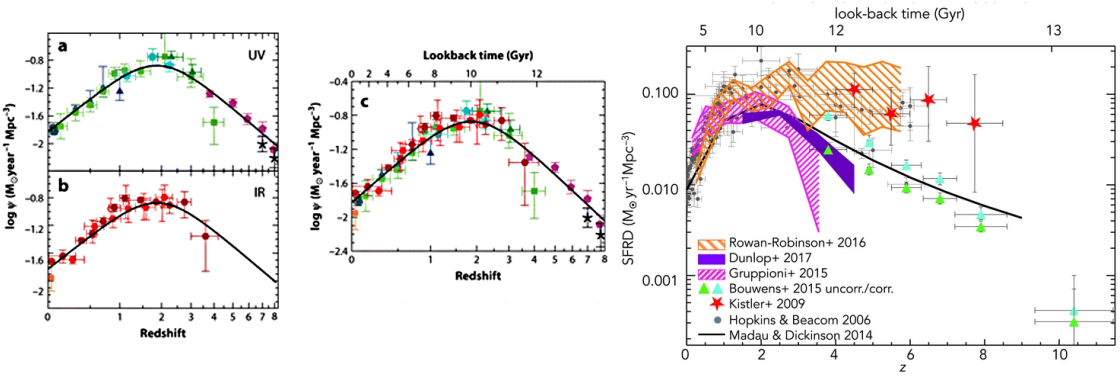

Figure 2.1: (left) The history of cosmic star-formation from (a) FUV, (b) IR, & (c) FUV+IR rest-frame measurementsc(Madau & Dickinson 2014). (right) Redshift evolution of co-moving SFRD. Different derivations of the obscured and unobscured SFRD are compared (Gruppioni et al. 2017)

between the radio and infrared emission, both of which are related to star-formation; the infrared emission emanating from dust heated by photons from young stars, whilst the radio emission arises from synchrotron radiation due to the acceleration of charged particles produced in supernova explosions. Deep radio surveys of the sky are able to detect many thousands of faint, star-forming galaxies out to several redshifts and allow a definitive radio-based, and hence obscuration-free, census of the star-formation rate history of the Universe – provided that radio emission from AGN-jet activity can be separated from that associated with star-formation.

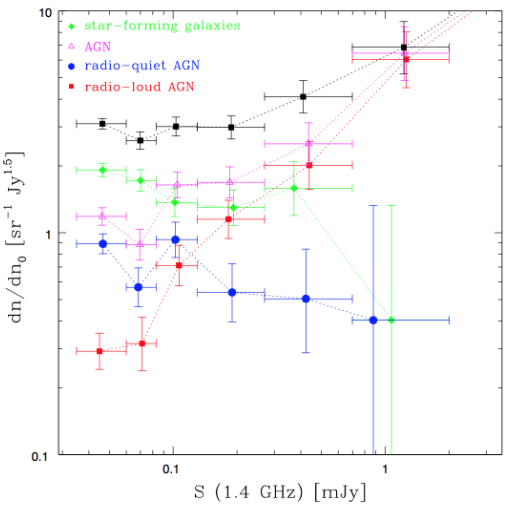

Figure 2.2: Euclidean normalised 1.4 GHz E-CDFS source counts for the complete sample (black filled squares) & various classes of radio source delineated by colour (Fig. 1, Padovani et al. 2015)

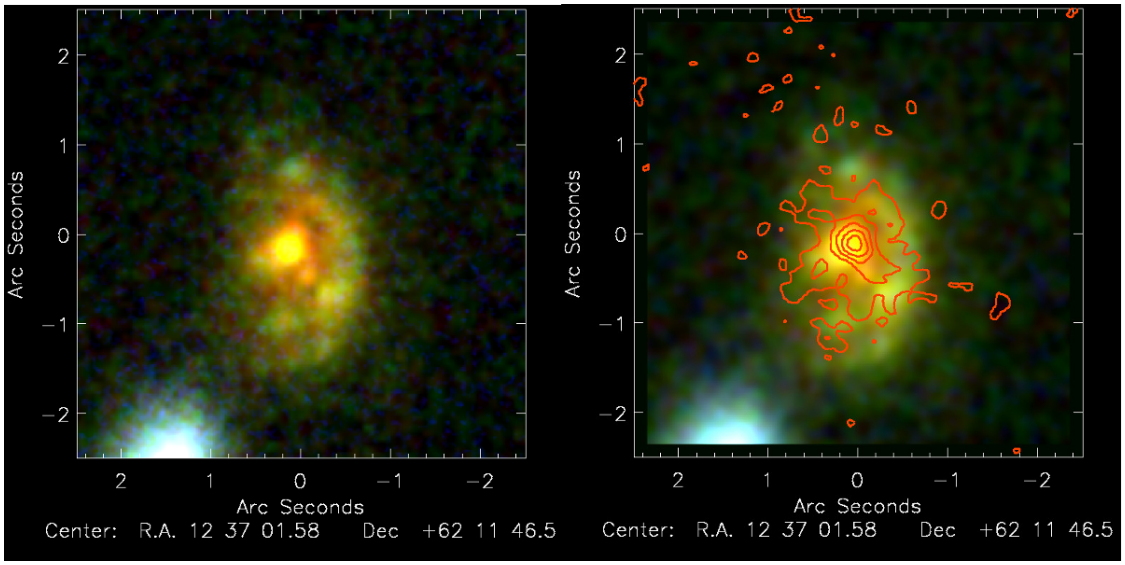

Figure 2.3: (left) Sub-mm very red dusty Seyfert galaxy GN17 at $z = 1.76$. S-F rate $\sim$720 $M_{\odot}$/yr. Possible extended SFG with a nuclear starburst. (right) *e*-MERLIN+JVLA 1.4 GHz image overlaid CI=4.5 μJy/bm (Beam 280 $\times$ 262 mas). Courtesy of Tom Muxlow.

2.1.2 Nature of the Faint Radio Population

At low 1.4 GHz flux densities the radio source population evolves significantly with star-forming galaxies starting to dominate the source counts over radio-loud AGN at flux densities below 100μJy. In addition, radio-quiet AGN systems begin to dominate the AGN population detected as shown in Figure 2.2 from Padovani et al. (2015) from deep VLA observations of a sample of radio sources in the Extended *Chandra* Deep Field-South. Padovani et al. identify the radio-loud AGN population as associated with 'jet mode' accretion with bright compact cores and extended radio jet structures on sub-galactic scales; and the radio-quiet AGN with 'radiative mode' accretion, the local luminosity function of the latter being not inconsistent with Seyfert galaxies. Star-forming galaxies clearly dominate the radio populations at μJy flux density level and contain steep-spectrum extended radio components on sub-galactic scales. Similar extended radio emission is also seen in many of the radio-quiet sources indicating that the radio emission in such systems may also be dominated by that generated in star-formation processes with AGN activity mainly detected in wavebands other than the radio. However, the high resolution radio imaging to date shows a variety of radio structures for the radio-faint AGN population with the implication that the population is heterogeneous and that higher angular resolution still is required to reliably separate any embedded AGN-jet structures from extended radio emission from star-formation regions across the host galaxy.

Separating AGN and star-formation related radio emission

VLBI with mas-scale angular resolution has historically been used as a definitive tracer of radio-loud AGN activity with its ability to identify very high brightness temperature compact core radio components associated with AGN 'jet-mode' accretion activity, together with the inner extended jet components ejected from such activity. Sub-arcsecond resolution imaging from compact VLBI arrays such as *e*-MERLIN, and the JVLA at higher frequencies, have been used to resolve and separate AGN-jet structures from extended regions of star-formation in a number of multi-band deep

fields (e.g. Richards et al. 1998, Chapman et al. 2003, Morrison et al. 2008, Smolčić et al. 2017) allowing obscuration-free estimates of star-formation rate (SFR) to be derived. The high resolution imaging has also shown that luminous star-forming galaxies (SFGs) are likely to contain compact nuclear starbursts in addition to extended regions of star-formation. These nuclear starbursts are resolved by *e*-MERLIN at L-Band (Muxlow et al. 2005) and the JVLA at 10 GHz (Murphy et al. 2017), but not detected by VLBI at mas resolution to present sensitivity levels. Murphy et al. find that the median FWHM size of the nuclear starbursts from a sample of 32 SFGs at 10 GHz in GOODS-N is $\sim$170 mas, whereas *e*-MERLIN+JVLA 1.5 GHz imaging shows both the nuclear starbursts in addition to extended steep-spectrum star-formation related emission with resulting median angular size values of $\sim$1.2 arcsecond. Some such systems are also associated with AGN activity in other wavebands (e.g. X-rays, optical broad-lines), complicating the radio source classification within the scheme shown in Figure 2.2, blurring the division between the SFG and radio-faint AGN populations. This issue is illustrated in Figure 2.3 where the z=1.76 dusty sub-mm galaxy GN17 identified with the *Scuba* source HDF 850.6 has historically been interpreted as a system undergoing a burst of intense star-formation through SED fitting from modified local ULIRG profiles (e.g. Pope et al. 2006). The faint *Chandra* X-ray detection also favours star-formation rather than an AGN interpretation. The sub-mm and IR emission from GN 17 indicate very significant reprocessing of UV radiation by dust; however, in spite of the large amount of dust obscuration, GN 17 possesses a bright optical nucleus and the 270mas resolution radio image shows a morphology which could be interpreted as either an extended SFG with a resolved nuclear starburst or a SFG with an embedded AGN-jet system. The relatively compact radio component overlies the bright optical nucleus, is not detected by the EVN at mas resolutions, and possesses a brightness temperature (T_B<10^3K) - well below that expected for a radio-loud AGN core - so the SFG interpretation remains the most likely, but it is unclear what contribution UV radiation from the bright optical nucleus makes to the IR flux density of GN 17.

Intermediate resolution imaging between full VLBI and *e*-MERLIN angular resolutions is required to investigate in detail the radio structure of GN 17 and many other potential SFG/AGN hybrid systems seen in deep radio fields - and thus estimate any potential AGN contamination to the SFG radio flux densities. The EVN has pioneered combination imaging with *e*-MERLIN, and recent developments have allowed full integration of *e*-MERLIN antennas into the EVN, permitting radio imaging over such intermediate angular scales between 30 - 150 mas. Such imaging will also investigate AGN feedback on the detailed structure of the high luminosity SFGs nuclear starbursts in the presence of AGN active in other wavebands - in addition to resolving and imaging any embedded faint AGN-jet radio components which may also be present and contributing to the feedback processes.

The Faint Radio-Loud AGN Population

The radio structures of the μJy radio-loud AGN population as imaged with *e*-MERLIN+JVLA at L-Band (Muxlow et al. (2005), *e*-MERGE Consortium - private communication) show that both one- and two-sided extended radio structures are seen on sub-galactic scales associated with a central active compact AGN radio core (See Figure 2.4). This is in contrast to the classical double structures found on either side of the host galaxy which are typically associated with radio-loud AGN sources with 1.5 GHz flux densities $\gtrapprox$ 1mJy. Such systems may be young emerging AGN, or perhaps sources where the radio jets are disrupted by entrained circum-nuclear material in the nuclei of host galaxies that have yet to be swept clear of star-forming gas and dust by AGN activity. In GOODS-N the *e*-MERGE sub-arcsecond study of radio-loud AGN sources identifies the brighter μJy examples of the population from both spectral properties and EVN detections at full mas resolution of bright

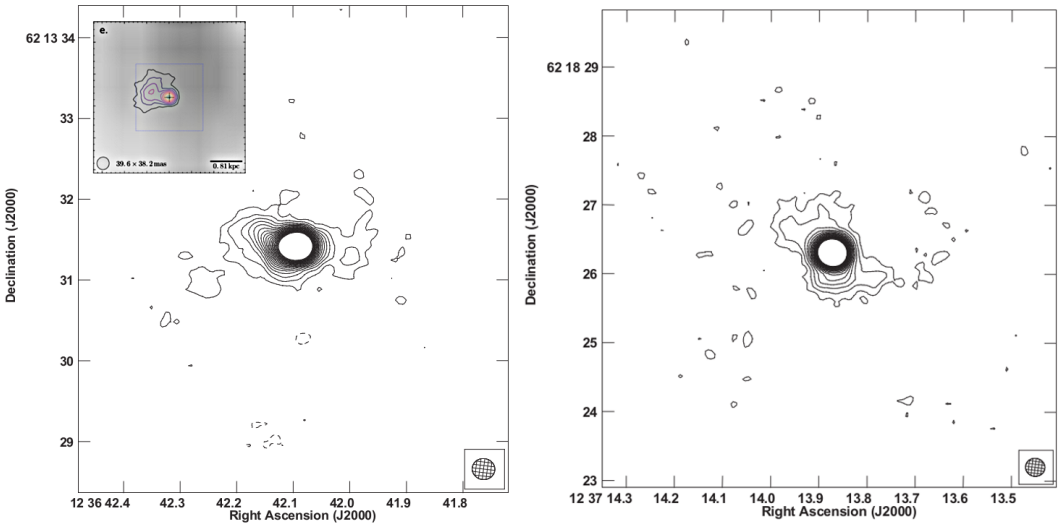

Figure 2.4: *e*-MERLIN+JVLA L-Band images (*e*-MERGE Consortium) of the faint μJy radio-loud AGN systems J123642+621331 (left) & J123713+621826 (right) showing 2-sided jet emission on arcsecond scales. Insert for J1213642+621331 displays an EVN+MERLIN combination image showing initial one-sided core-jet structure on $\sim$100 mas scales, imaged with a beam of 40×38 mas (Jack Radcliffe, private communication).

core components with brightness temperatures $>10^5$K (Chi, Barthel & Garrett 2013, Radcliffe et al. 2018). This selection favours systems aligned to the line-of-sight and thus initial one-sided jet structures would be expected if the jets are moving with relativistic velocities. Any jet entrainment from circum-nuclear material would result in disruption of the jet flow and deceleration of the jet plasma resulting in the appearance of two-sided jets. Intermediate resolution EVN+*e*-MERLIN imaging on scales of 10s of mas at L-Band are required to investigate the scales on which jets are one- or two-sided and the implied scales on which the initially one-sided jets are slowed. In Figure 2.4 (left) the insert image from archival VLA and MERLIN L-Band data demonstrates that for J123642+621331 the jet starts off one-sided and becomes two sided on scales between $\sim$100 - 250 mas ($\sim$0.8 - 2 kpc).

In recent years VLBI instruments have been employed to investigate a high redshift population of infra-red faint radio sources (IFRS) (e.g. Middelberg et al. 2008, Herzog et al. 2015). IFRS objects are thought to be radio-loud AGN systems at redshifts >2, and to be important probes into the co-evolution history of SMBH growth and galaxy assembly. Although VLBI observations have confirmed the presence of active AGN in many IFRS objects it remains unclear as to the nature of the extended radio emission also present in these sources. Intermediate resolution imaging on 10s of mas resolution scales is required to characterise the true nature of this class of object and to confirm that the radio emission is wholly associated with AGN activity.

2.1.3 Star-formation and accretion in the local Universe

At high redshifts, VLBI observations of galaxies can pinpoint the location of compact AGN related emission; however in the local Universe sensitive VLBI experiments can be used to investigate the detailed physics of star-formation and accretion in individual objects on linear scales matching the

physical processes, e.g. sub-parsec scales. In such a scenario each galaxy provides an individual laboratory of accretion powered sources such as AGN, as well as rapidly evolving stars, enshrouded by gas and dust, all of which are essentially at the same distance. The high angular resolution and sensitivity of interferometers are ideally suited to detailed studies of these objects - providing a unique probe to the physics of compact objects such as AGN. Supernovae and their evolving remnants probe the content and dynamics of the cool, neutral, and molecular ISM via molecular masers and absorption experiments at the highest angular resolution.

Supermassive black-holes exist at the centres of all galaxies, but only a fraction of these are in active states of accretion at any one epoch. This accretion is one of the most significant energy sources in the Universe, with the potential to clear star-forming gas from the galactic bulge area and regulate the growth of whole galaxies in clusters (e.g. di Matteo et al. 2015). This mechanical feedback mechanism through jets and outflows (see Section 3.1.3) is powered by the central accretion processes. Whilst the role and influence of accretion in luminous AGN sources has been well studied (see Chapter 3), comparatively little is known about the accretion activity of supermassive black-holes at low radiative luminosities, despite both their ubiquitous nature and importance to galaxy growth and evolution.

The low radiative efficiency of low-luminosity AGN, which are also commonly embedded in nuclear star-formation regions, means that the use of optical or X-ray diagnostics becomes increasingly challenging. However, sensitive, high resolution (sub- to milli-arcsecond angular resolution) radio observations can provide a direct probe of the jet power (see Fig. 2.5) hidden to other wavebands, and hence its mechanical influence on feedback (Nagar, Falcke & Wilson 2005). VLBI facilities have a critical role in such studies (e.g. Baldi et al. 2018; Park et al. 2017; Pérez-Torres et al. 2010) by reaching sensitivities of a few 10s of μJy they can probe the equivalent X-ray flux (applying the 'fundamental plane' relation for accreting black-holes, e.g. Falcke, Körding & Markoff 2004) of 10^{38} erg s^{-1} for a 10^7 M$_\odot$ black-hole at 20 Mpc, which is a factor of 20 lower than the typical equivalent [OIII] detection limit of traditional optical spectroscopic surveys. Over the coming decade sensitive, milliarcsecond resolution combined VLBI and *e*-MERLIN surveys of the compact core emission, and importantly the imaging of the inner jet structure, from samples of low-luminosity AGN will provide a unique characterisation of the SMBH accretion activity in the local Universe, allowing the links to SMBH activity with other galaxy properties and putting SMBH activity in the wider context of its implication on black-hole growth, and the regulation of galaxy evolution via feedback.

Beyond the most massive systems, accretion remains a dominant process across a range of black-hole system masses down to intermediate-mass and stellar-mass black-hole systems. Outside our own Galaxy such accreting systems are commonly seen as off-nuclear Ultra Luminous X-ray (ULXs), or microquasars/X-ray binary (XRBs) sources in many local galaxies, but are typically faint at radio wavelengths and only detectable in the most extreme cases and in the deepest VLBI observations. By their nature these are associated with the endpoints of massive star-formation.

In the case of extragalactic microquasars an extrapolation of the radio characteristics from galactic equivalents (see Chapter 4) are expected to be compact, highly variable objects which may show superluminal motion. Within nearby star-forming galaxies ($<$100 Mpc) VLBI has thus shown tentative evidence for persistent and variable emission from such sources in a few cases, notably in Arp 220, Arp 299 and M82 (Batejat et al. 2012; Pérez-Torres et al. 2009; Muxlow et al. 2010) with detections of variable and superluminous sub-mJy radio sources. Persistent radio emission from an ULX source, NGC 2276 3c, was tentatively reported on milliarcsecond scales (ULX NGC 2276 3c, Mezcua et al. 2015) revealing compact jets 1.8 pc within its larger, 650 pc radio lobe with the EVN.

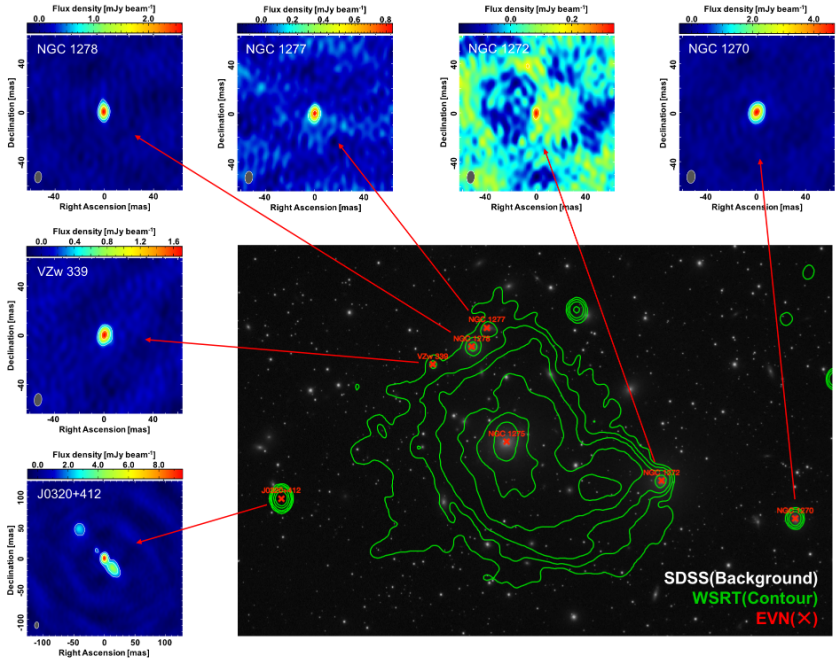

Figure 2.5: Combined image of the radio-optical images with compact radio sources detected from the EVN observation on a mas scale. The green contours represent the 1.4-GHz WSRT radio continuum that is overlaid on an SDSS g-band image (Fig. 1, Park et al. 2017).

This result remains at the cusp of current capabilities (Yang et al. 2017). Such studies are at the limit of existing VLBI arrays and limited to the most luminous examples in their class. However, advances in the sensitivity and capabilities of VLBI arrays during the coming years will open up the possibility of imaging many of these targets which will provide vital constraints on radio emission from the full mass range of black-hole systems across a range of galaxy types.

2.1.4 Star-formation processes

Characterising the star-formation history, along with the current level of star-formation, within individual and ensembles of galaxies remains a crucial physical parameter in understanding galaxy evolution. Equally important to our understanding is the role of massive stars and their subsequent stellar end points, on the surrounding ISM in galaxies and the part they play in self-regulation of the triggering and fuelling of both star-formation and accretion. Both within the local and distant Universe, much of the most intense star-formation activity occurs in the dust-enshrouded centres of star-forming galaxies, which are essentially invisible to traditional observational tracers of star-formation such as optical and even, in the most extreme cases, the infrared and X-rays. It is well recognised that the levels of both radio synchrotron and thermal Bremsstrahlung radio emission are excellent tracers of the large scale star-formation rates in galaxies (Beswick et al. 2015). However, the link between synchrotron emission and star-formation is via a complex physical mechanism, and the isolation of the fainter thermal free-free emission component requires detailed characterisation of the radio spectral energy distribution and/or the use of other a priori information such as optical recombination data (e.g. Westcott et al. 2018; Galvin et al. 2016).

Radio observations, and in particular high resolution (VLBI), provide a clean and fundamental tracer of the products of star-formation, such as supernovae (see Chapter 4) and supernova remnants, which is unbiased by obscuration. Whereas low resolution radio observations of star-forming galaxies trace the diffuse radio emission primarily originating from charged particles that have escaped old supernova remnants, high sensitivity VLBI+*e*-MERLIN observations can systematically detect, characterise and resolve individual radio supernova and their remnants on a galaxy by galaxy basis, critically resolving away the 'confusion' of the diffuse galaxy emission. By the characterisation of this population the highly obscured massive supernovae/star-formation rates of starburst and ultra-luminous galaxies can be directly inferred.

To date a number of such studies have been undertaken in individual galaxies (e.g. Varenius et al. 2019; Pérez-Torres et al. 2009; Bondi et al. 2012; Fenech et al. 2010). These have identified large populations 'supernovae factories' of compact radio sources with each galaxy effectively acting as a laboratory containing multiple discrete radio sources at different stages in their evolution, in different physical environments which all lie at essentially the same distance and can be studied in a systematic manner. One of the best studied example is the ULIRG Arp 220 (see Fig. 2.6, Varenius et al. 2019 and references therein) for which VLBI observations over the last two decades have detected nearly 100 compact radio sources including multiple new supernovae, supernova remnants and variable sources. The ultimate resolution that VLBI arrays provide has allowed a number of these sources to be resolved allowing new insights into the evolution of supernova remnants, as well as preferentially probing the top-end of the stellar initial mass function within the dense environments of these extreme starformers.

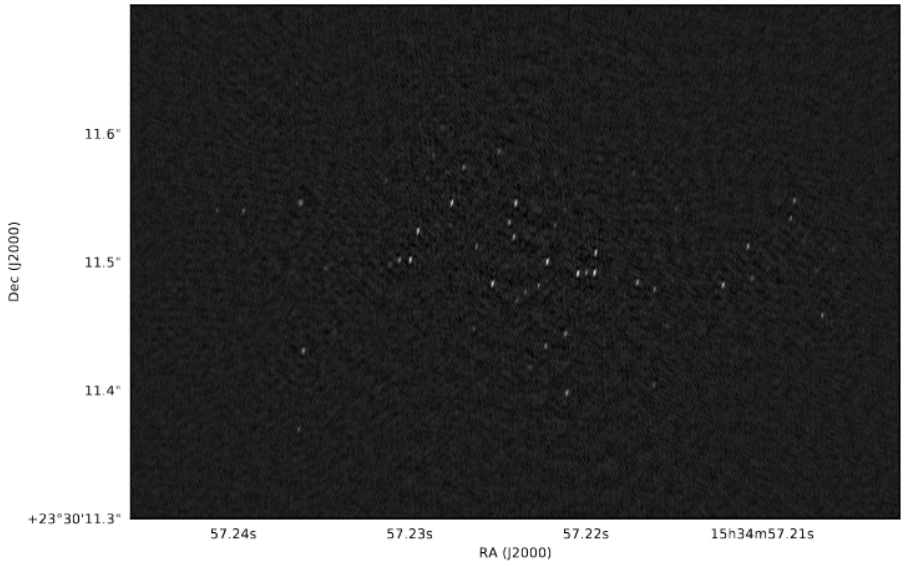

Figure 2.6: Deep (rms 4 μJy/b) 6 cm VLBI imaging of the western nucleus of Arp 220. Credit: Varenius et al. (2019), reproduced with permission ©ESO.

However, studies of these extreme star-forming local galaxies (e.g. Arp 220, Arp 299 and others) have implications beyond their important contributions to the physics of star-formation and stellar evolution within these individual galaxies. These extreme star-forming environments, with star-formation rates exceeding 1000s $M_\odot$ yr^{-1}, provide the best local Universe analogues available for

the sites of extreme star-formation in the optically-faint, dusty star-forming galaxies (e.g. sub-mm galaxies) in the distant Universe (see above). In the distant Universe observations do not have the spatial resolving power to unravel the individual compact source properties, whereas VLBI studies of these local analogues do. Such local galaxy studies are crucial in providing the key anchor point for our wider understanding and interpretation of cosmic star-formation evolution in galaxies at all redshifts.

2.1.5 Requirements and synergies (continuum)

Unique VLBI combination μJy sensitivity wide-field L-Band imaging on intermediate angular resolutions between 20 and 200mas is required to investigate the detailed radio structures of the SFG nuclear starbursts to determine how they differ from their low-redshift equivalents; to investigate any feedback from AGN activity in other wavebands; to characterise direct mechanical feedback from any faint embedded radio AGN-jet activity that may be detected in both the SFGs and diverse radio-quiet source population. Such studies are fundamental to accurately separate star-formation associated radio emission from AGN-jet contamination in deep-field investigations of the evolution of star-formation rate density with cosmic time - and demonstrate a new research area for wide-field VLBI in intermediate resolution studies of high redshift star-formation radio structures. They are also vital in assessing the role of AGN in promoting and controlling star-formation activity at high redshifts, and provide a link to understanding the co-evolution of SMBH growth with the assembly of galaxies in the early Universe. Intermediate resolution combination imaging of the faint μJy radio-loud sources at both L- and C-band will also characterise the jet properties of this new population, and investigate the role of the circum-nuclear environment in disrupting jet flow on sub-Galactic scales. Similar requirements apply for studying star formation and accretion in the local Universe. In addition, isolation of thermal free-free and synchrotron processes would benefit from very wide bands. Detailed studies of star formation product tracers (SNe) require (sub-)mas imaging at GHz frequencies.

2.2 Active Galactic Nuclei and their impact on galaxy evolution

After almost three decades of observations, more and more pieces of evidence call for a revision of the Unified Model of active galactic nuclei (AGN). The unification scheme proposed by Antonucci (1993) postulates that all AGN are intrinsically the same physical object and that the observed dichotomy between broad line (*type 1*) and narrow line (*type 2*) AGN is only due to the orientation relative to a dusty toroidal structure surrounding the nuclear engine (the “torus”) (Antonucci 1993; Urry & Padovani 1995). However, X–ray and IR studies have changed our view of the classical dusty torus, from a uniform isolated entity to a clumpy structure connected with the host galaxy via gas inflows and outflows (for a recent review see Ramos Almeida & Ricci 2017). Mid-IR interferometry has revealed that the emitting dust is concentrated on scales of 0.1–10 pc and, in most cases, can be modelled with two nuclear components, instead of a single disk or toroidal structure (Burtscher et al. 2013). The most recent models for IR emission in AGN imply an equatorial inflowing disk and a polar-extended structure, which may originate from a dusty outflowing wind (e.g. Hoenig & Kishimoto 2017). Despite the great progress made, whether the torus is geometrically thick, if the polar elongation is always present, and whether the broad line region (BLR) and the torus are produced by accretion disk winds are still a matter of debate.
The study of the physical properties, structure, and kinematics of the gas surrounding SMBHs is fundamental in answering these open-ended questions and in building detailed models of AGN.

These studies, however, are complicated by the extremely small spatial scales (less than 10 pc) and by the complex structures of the nuclear components. Moreover, particularly in type 2 AGN, the inner regions are often obscured at optical and UV wavelengths. Current X-ray and IR instruments can access these regions but are not able to resolve them, and information on their structure have to be inferred by modelling the emitted radiation. The radio emission can penetrate the large column densities of gas and dust that often obscure the line of sight to the nucleus. In particular, at radio wavelengths, studies of luminous water and hydroxil masers (traditionally referred to as "megamasers") permit to directly map the molecular gas at tens of parsec or even at sub-parsec distances from the SMBH. Indeed, the high brightness temperature and small size of the maser spots make them perfect targets for Very Long Baseline Interferometry (VLBI) observations, through which angular resolutions of the order of 0.1 mas can be reached.

2.2.1 Extragalactic studies with masers and megamasers

Extragalactic OH masers are typically observed at the rest frequencies of 1665 and 1667 MHz, corresponding to the first two of the four hyperfine transitions of the ground rotational levels of the molecule (for recent reviews see e.g. Lo 2005; Tarchi 2012). These masers are typically associated with starburst regions within a few hundred pc from the nucleus and have luminosities intermediate between Galactic stellar masers and extragalactic megamasers which are associated with AGN activity. In only two cases (Mrk 231 and IIIZw 35) OH emission, mapped with VLBI, appears to be related to AGN activity, tracing a rotating dusty structure located between 30 and 100 pc from the nuclear engine and a parsec-scale ring, respectively (Kloeckner, Baan, & Garret 2003; Pihlstroem et al. 2001). Hydroxyl masers are used to investigate the gas dynamics in star-forming regions.

VLA studies of hydroxyl maser emission within the central kiloparsec region of the nearby (D=3.7 Mpc) starburst galaxy M 82 (Argo et al. 2010) detected 13 masers distributed across the central 30 arcseconds. Whilst remaining spatially unresolved, several of these masers show significant velocity structure indicating that such masers are associated with multiple masing regions within the beam along the line of sight. The masers can be used to investigate the distribution of the molecular and atomic gas present in the nuclear region of M 82 by overlying a position-velocity ($p-v$) plot of the molecular hydroxyl masers on the atomic H I absorption. The comparison plot is shown in figure 2.7 which is aligned along the major axis of M 82 where the 1667 MHz masers are contoured over the H I absorption seen in the atomic gas in grayscale; the H I absorption being derived from 1420 MHz data from the VLA archive (programme AW444; Wills et al. 2000).

The distribution of the masers is well correlated with the H I absorption with the rotation of the nuclear region of M 82 shown running ∼linearly from top left to bottom right. However, it is clear that there is an additional blue velocity arc running from the galaxy centre which contains both atomic and molecular gas with several of the brightest masers located on the arc. This feature has been suggested to be either an expanding super-bubble or the x_2-orbits of an inner bar (Wills et al. 2000).

EVN observations of two masers within the blue arc (Argo 2018), spatially resolve the masing regions and show a significant difference in line ratios for the different spatial components within the masing regions. These main-line OH masers are radiatively pumped and collisional de-excited to the rotational ground state with the line ratios being dependent on the physical conditions within the masing cloud (Gray 2007) – see figure 2.8. Thus high resolution imaging of hydroxyl masers can act as a detailed probe of the physical conditions within the masing regions in nearby star-forming galaxies.

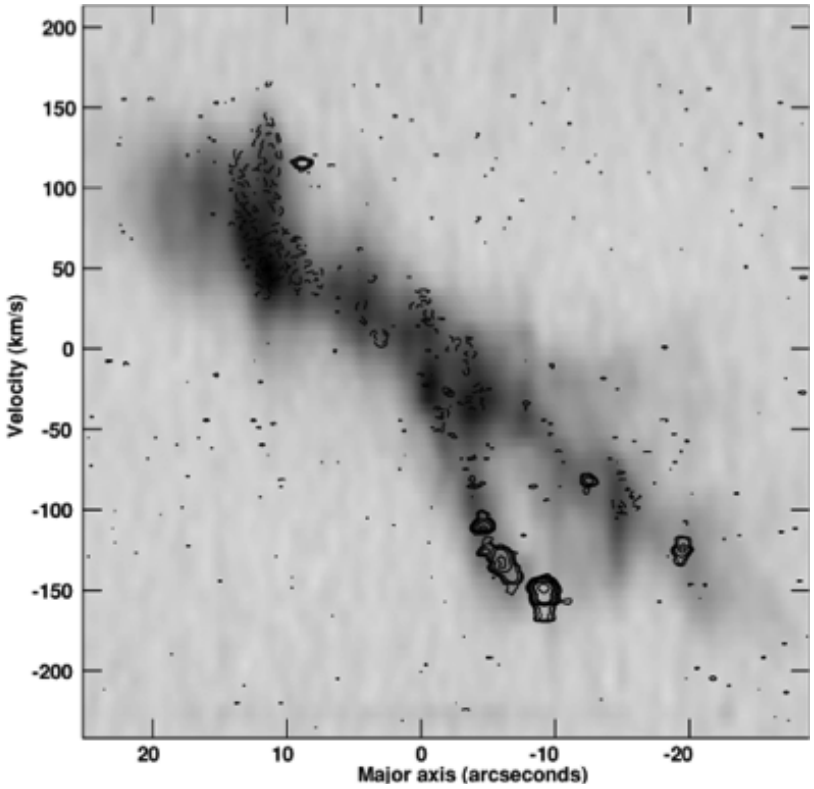

Figure 2.7: 1667 MHz masers contoured over H I absorption (grayscale). Offsets from dynamical centre & velocity relative to systemic (225 km s^{-1}). From Argo (2018).

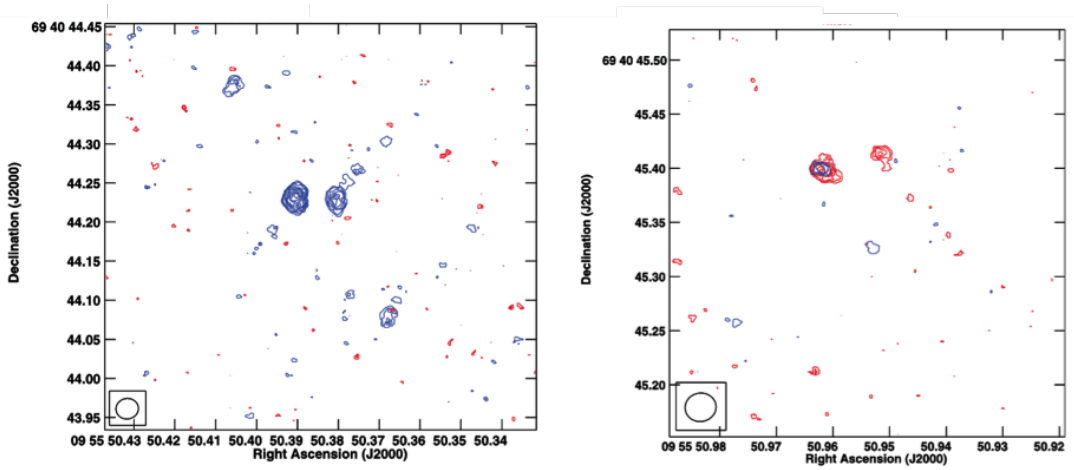

Figure 2.8: Comparison of the 1667 MHz (blue) and 1665 MHz (red) and emission for the masers 50.37+44.3 (left panel) and 50.95+45.4 (right panel). From Argo (2018).

In the remainder of this section, we will focus on water megamasers that, differently from hydroxil ones, have always been found to be associated with nuclear activity. The 22 GHz maser line of ortho-H_2O may trace three distinct phenomena related to AGN. Typical triple-peak line systems are associated with edge-on accretion disks. VLBI and single-dish monitoring studies of disk-masers allow us to map accretion disks and to determine the enclosed dynamical masses (e.g. Kuo et al. 2011; Gao et al. 2017; Zhao et al. 2018). In addition, radio continuum observations of disk-maser galaxies have recently been used to test some aspects of the AGN paradigm, that is, the alignment between the radio jet and the rotation axis of the accretion disk (Kamali et al. 2019, and references therein). H_2O megamasers may also trace nuclear ejection processes in the form of jets or winds. Indeed, they have been found to be associated with the interaction of the jets with molecular clouds in the host galaxy (Gallimore et al. 2001; Peck et al. 2003; Castangia et al. 2019) or with wide-angle outflows at less than 1 pc from the nuclear engine (Greenhill et al. 2003). Observations of the best-studied jet-maser, in Mrk 348, using the reverberation mapping technique, provided estimates of relevant physical quantities such as the jet velocity, the shock speed, and the densities of the material in the jet and in the ambient medium (Peck et al. 2003). Water maser observations in Circinus (Greenhill et al. 2003) and NGC 3079 (Kondratko et al. 2005), instead, seem to have resolved individual outflowing torus clouds at <1 pc from the nuclear engine, probing the geometry and kinematics of nuclear winds. Therefore, each megamaser source provides a plethora of information on the (sub-)parsec-scale environment around AGN, making the discovery of new sources and their interferometric follow-up extremely important for AGN studies.

Very bright masers (with peak flux densities of the order of 1 Jy) as, for example, the ones in NGC 4258, NGC 3079, and NGC 1068 can be observed with any existing VLBI array. On the contrary, high angular resolution observations of weaker but still relatively bright masers (with peak flux densities from tens to hundreds of mJy) require sensitive instruments like the VLBA and the EVN, capable of reaching rms of a few mJy per 0.2 km/s channel within a few hours on-source. This is essential to image the largest possible number of maser spots and Doppler components, whose spectral linewidths can be as narrow as 1 km/s or less. The weakest masers, with peak flux density up to 10 mJy, instead, can be observed only with the most sensitive arrays like the High Sensitivity Array (HSA), or Global VLBI. The EVN may play an important role in extragalactic maser studies, since with the inclusion of large antennas (e.g. the new 64-m Sardinia Radio Telescope) the sensitivity of the full array at 22 GHz is much higher than that of other VLBI arrays. However, in order to fully exploit this enhanced feature, the frequency coverage of the receivers available at each station has to be as homogeneous as possible. For example, at K band, the water maser line (rest freq. 22.23508 GHz) in a galaxy with recessional velocity of 10000 km/s (z$\sim$0.03) would be detectable at $\sim$21.5 GHz. If the K-band receivers of a number of stations do not cover this frequency, the VLBI array usable for observing such a transition would turn out to be incomplete, with an impact (significant, in some cases) on the final sensitivity and *uv*-coverage of the measurements.

2.2.2 Outflows and AGN feedback

Hydrogen is the most abundant element in the Universe occurring in different phases in various structures that cover a range of spatial scales. The radio regime is particularly well suited for the study of neutral atomic hydrogen (H I), because of the hyperfine transition at 1420 MHz (or 21 cm). H I provides a wealth of information on the nature of gaseous matter in the Universe which is why it has been identified as one of the key science drivers for the SKA (Staveley-Smith & Oosterloo 2015; Morganti et al. 2015) and its precursors.

In general, H I can be observed in *emission* and *absorption*. However, only connected interferometers or single-dish telescopes have the brightness temperature sensitivity to detect H I emission, mostly in the nearby Universe. The situation is different for H I absorption, which only requires a radio background source (often a radio AGN) and a sufficient optical depth[1] of the gas.

It is common to distinguish two types of H I absorption: *intervening* and *associated* absorption. In the former case, the observed gas and background source belong to two independent systems. This allows the study of H I gas in a galaxy (even our own) which is in front of a more distant active galaxy along the observer's line of sight. As such, intervening absorption can be used to trace the gas content over a range of redshifts which gives insight into evolution of galaxies in the Universe (Curran 2017). In case of *associated* absorption, the observed gas and background source are located in the same system, e.g., the same galaxy and the gas has to be in front of the background source. This constraint is a great benefit, because it allows to deduce the kinematic structure of the gas, e.g., whether it is regularly rotating, infalling or outflowing gas. This is particularly interesting for the understanding of feeding and feedback in radio AGN. Several studies have also shown a higher detection rate of H I absorption in young and restarted AGN which could be related to a denser ISM and may provide insight into the evolution of AGN (e.g. Morganti & Oosterloo 2018). A vital step in understanding the gas dynamics is to resolve the distribution and kinematics of the gas close to the AGN. In most cases, this requires reaching sub-kiloparsec scales and sub-arcsec angular resolution which can be provided by VLBI. Almost no other observing technique can acquire information on the gas content of a galaxy on these small spatial scales.

Systematic searches for H I absorption are generally conducted with lower-resolution interconnected interferometers or single-dish instruments. The upcoming large surveys planned with SKA pathfinders and precursors promise a major increase in the number of H I absorption using "blind searches" (see Table 2.1), thanks to the large instantaneous band. This will open up the possibility of statistical studies of the properties of the H I gas in larger and new groups of sources. The follow-up with VLBI will be a key addition in order to maximise the science, in particular in the SKA era when VLBI with the SKA promises a significant boost in sensitivity.

Other sources of associated H I absorption are star forming galaxies and supernova remnants (e.g. Muxlow et al. 2006; Leahy & Tian 2010), but the largest contribution of H I VLBI continues to be AGN studies. Thus, the majority of this chapter will focus on this topic. Intervening absorption studies with VLBI may become more prominent in the future (e.g. Biggs et al. 2016; Gupta et al. 2018).

2.2.3 Tracing neutral atomic hydrogen on parsec scales

H I VLBI has a long tradition and a range of studies have shown how tracing H I on parsec-scales reveals a variety of gas structures in the close surroundings of the central supermassive black hole. Here, we highlight only some recent results. Particularly important are the studies of the presence of H I in tori and circumnuclear disks. These structures are considered a key ingredient in AGN, affecting the view of the central regions and providing a reservoir of gas for the fueling of the central engine. Recent theories predict them to be clumpy and perhaps even warped (Ramos Almeida & Ricci 2017). In particular in radio galaxies, VLBI has provided important information (see e.g. Araya et al. 2010; Morganti & Oosterloo 2018 for an overview). Struve & Conway (2010) confirmed the presence of a nuclear disk in Cygnus A using the VLBA (see Fig. 2.9). The disk is located

[1] The optical depth τ is defined as $\tau = \log(1 - \Delta S_{\rm abs}/(c_f S_{\rm cont}))$ where $\Delta S_{\rm abs}$ is the absorbed flux density, $S_{\rm cont}$ the continuum flux density, and c_f the covering factor.

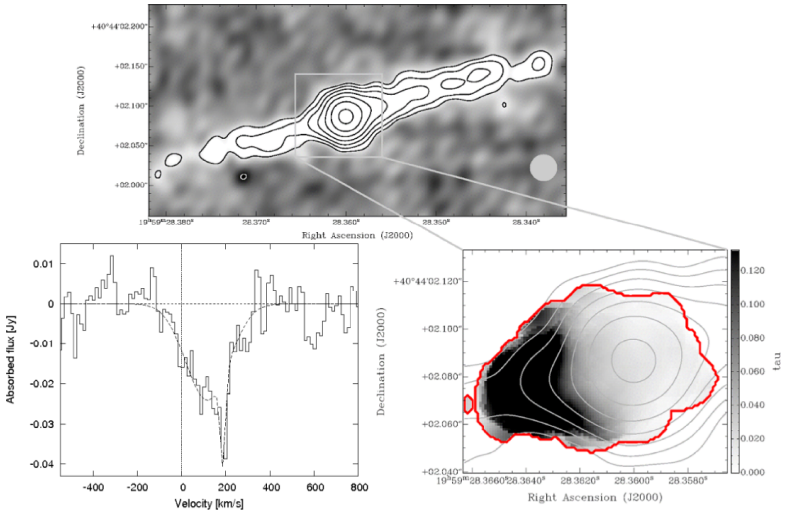

Figure 2.9: The circumnuclear disk of H I gas detected towards the central few parsec in Cygnus A. Credit: Struve & Conway (2010), reproduced with permission ©ESO.

at a radius of about 80 pc, has a scale height of about 20 pc and a density of $> 10^4\,\mathrm{cm}^{-3}$. Espada et al. (2010) detected absorption in Centaurus A about 0.4 pc away from the nucleus which could be part of a circumnuclear disk, but this is not yet confirmed. In the restarted, giant radio galaxy 3C 236 a thick disk of H I gas is observed at radius of about 880 pc and a scale height of at least 400 pc (Schilizzi et al. 2001; Struve & Conway 2012; Schulz et al. 2018). The orientation of the disk coincides with a dust-lane and a disk of ionised and molecular gas. Struve & Conway (2012) also suggested the existence of an almost edge-on disk or torus with a radius of < 200 pc in 4C 31.04. H I gas has also been detected in absorption in the centre of cool-core galaxy clusters. The limited available data have shown that the gas may be concentrated in tori-like structures.

Another important finding is that not all the gas is settled in regularly rotating structures. The search for infalling gas fueling the AGN has been particularly difficult with only a few cases where, thanks to the high resolution of VLBI, this gas could be identified and separated from the settled gas. In PKS $2322-123$ located in the X-ray cooling cluster Abell 2597, Taylor et al. (1999) detected narrow redshifted absorption indicative of infalling gas in addition to a torus-like structure of H I. A similar situation has been reported for J094221.98+062335.2 which belongs to a galaxy pair that is undergoing a major merger (Srianand et al. 2015). VLBI observations of the central radio emission of the giant radio galaxy NGC 315 spatially resolved H I gas that is likely falling towards the centre of the AGN (Morganti et al. 2009). Other examples are $B2352+495$, 4C31.04, PKS $B1718-649$ and the cluster Abell 2597 (Araya et al. 2010; Struve & Conway 2012; Tremblay et al. 2016; Maccagni et al. 2017). In the latter two cases, the infalling gas has been linked to chaotic cold accretion processes (see also Fig. 2.11).

Finally, the most recent and surprising finding is that H I is also involved in AGN-driven fast outflows. A striking signature of this phenomenon is the presence of broad blueshifted absorption of H I covering up to 1000 km s^{-1}. This has been detected in a number of different AGN such as young or restarted radio galaxies, but also Seyfert galaxies (see Morganti & Oosterloo 2018 for a review). The powerful resolution of VLBI has made it possible to trace the outflows down to parsec-scale.

Morganti et al. (2013) detected a massive $> 10^3 M_\odot$ outflow in 4C 12.50 towards the southern radio lobe about 100 pc away from the nucleus. More recently, Schulz et al. (2018) partially recovered the H I outflow in 3C 236 with VLBI. Rather than a single, slightly extended feature as in 4C 12.50, the outflow seems to be clumpy. The highest velocity clouds are compact and are detected towards the nuclear region while an extended feature is also detected co-spatial to the lobe (see Fig. 2.10). These results indicate that at least in some cases the H I outflows are driven by the jet as it enters a clumpy medium. In other cases the outflowing gas is still likely to be clumpy, but driven by radiation pressure (e.g. Mrk 231, Morganti et al. 2016). The location of the outflow with respect to the radio source provides the best way to distinguish between these driving mechanisms (e.g. Morganti et al. 2013). Interestingly, H I outflows have been predominantly detected in young and restarted radio galaxies.

2.2.4 Probing AGN feedback and galaxy evolution with VLBI

Observationally, H I VLBI continues to have a tremendous astronomical impact by utilising the full spectral power of VLBI. A single observation provides not only information on the gas properties but vital complementary data on the continuum source. As such it requires dealing with the particular challenges in calibration, RFI mitigation and data processing. In addition, it is well suited for wide-field observations which require high spectral and time resolution. H I VLBI affects the design of current and future generations of telescopes. As such, it will play an important role in utilising the full potential of VLBI observations with the SKA.

The data itself is vital to constrain theoretical models and numerical simulations of AGN feedback and evolution on galactic scales (Mukherjee et al. 2016, 2017, 2018). Even though these simulations do not fully model the cold gas, in many cases H I VLBI is the only observational technique which can match the resolution of the simulations. This provides at least a qualitative comparison which is particularly important for studying inflows and outflows of gas.

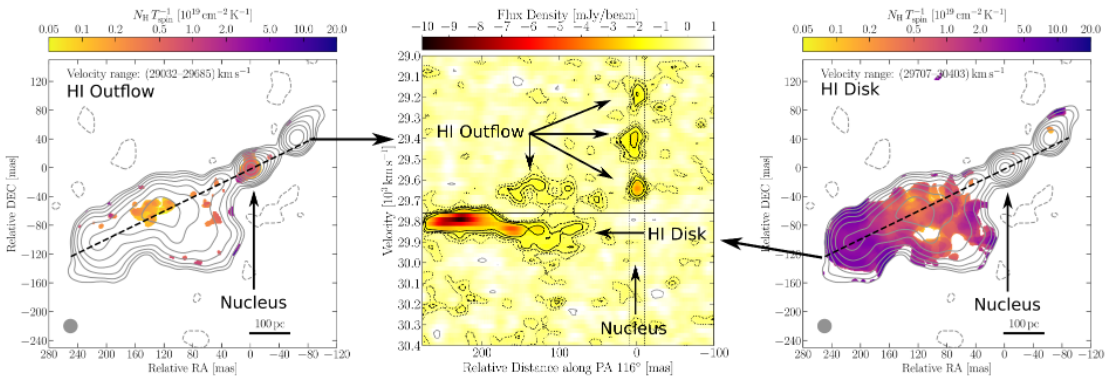

Figure 2.10: The jet-driven outflow of H I gas in 3C 236 has been partially recovered with VLBI revealing a clumpy structure even towards the nuclear region of the AGN. Adapted from: Schulz et al. (2018), reproduced with permission ©ESO, and Morganti et al. 2018b.

H I studies with the EVN

So far, H I absorption studies have been limited to a few case studies. This will change in the coming years with the upcoming H I surveys conducted around the world (Table 2.1). They will significantly expand the sample of known H I systems. In the northern hemisphere, the SHARP survey conducted

Survey	Redshift range	Noise over 5 km/s [mJy/beam]	Sky coverage [deg^2]	Number of detections	Detection limit [mJy]
APERTIF-SHARP	0–0.26	1.3	4000	400	30
ASKAP-WALLABY	0–0.26	1.6	30000	2300	40
MeerKAT-MALS	0–0.57	0.5	1300	450	15

Table 2.1: Overview of upcoming H I absorption surveys taken from Morganti & Oosterloo (2018).

by APERTIF will likely become the reference catalogue for H I VLBI follow-up with the EVN. The detection rate of H I has been estimated for radio galaxies to be 20%–30% (e.g. Maccagni et al. 2017; Curran & Duchesne 2018). Southern hemisphere surveys will also cover areas of the sky accessible to the EVN. VLBI follow-up observation will yield important high-spatial resolution information of associated absorption in a significantly larger number of sources. This will open the possibility of an unprecedented statistical analysis of the properties of H I gas covering a variety of radio AGN. The results will shed light on the gas dynamics for different types of AGN and their evolution.

The upcoming surveys will also provide a larger sample of intervening absorption. Thus, H I VLBI will be used to gain information on the gas structure of these absorbers (see e.g. Biggs et al. 2016; Gupta et al. 2018 and references therein). As these system are likely non-active galaxies, the data will help understand the evolution of galaxies.

It is less clear whether H I VLBI will become more important for studies of starburst galaxies and supernova remnants, because of the required sensitivity.

There are technical as well as scientific limitations to the study of intervening and associated H I in absorption. The technical limitations are specific for VLBI. The frequency range covered by L-band receivers on VLBI telescopes limits the redshift range to $\lesssim 0.12$. As a result, only a subset of sources detected by upcoming surveys can be followed-up. In addition, since the EVN is a heterogeneous array, not all L-band receivers are able to reach this value while others are technically capable of going to lower frequencies (e.g. *e*-MERLIN). This limits the sensitivity of an observation. As there are no plans to extend to lower frequencies, H I VLBI observations with the EVN will remain focused on the nearby Universe. However, there is an opportunity to significantly improve the scientific output in light of the developments for VLBI with the SKA which may be usable as a VLBI element at frequencies well below 1 GHz.

Another limiting factor is RFI, but its impact can vary. RFI can have a larger affect on short spacing than on longer baselines where it may correlate out. The RFI environment also changes from station to station. On the one hand, this makes RFI mitigation more challenging. On the other hand, it makes it possible to gain information for channels affected by RFI for some stations, by using the data from other stations at a similar spacing.

The scientific limitations are inherent to the nature of H I absorption experiments (e.g. Morganti & Oosterloo 2018 for recent overview). Only gas in front of the radio source can be seen, but this is also a benefit as it allows to differentiate between rotating, infalling and outflowing gas. With a few exceptions, associated absorption is limited to radio-emitting AGN. This is also the case for intervening absorption to some extent, as a background source (even a distant one) is still required. The main uncertainty is the spin temperature which is necessary to calculate the column density[2] and several other properties such as density, mass and other quantities. It is influenced by a range of

[2]The column density $N_{\rm H\,I}$ is defined as $N_{\rm H\,I} = 1.82 \times 10^{18} T_{\rm spin} \int \tau(v) dv$, where $T_{\rm spin}$ is the spin temperature.

effects (e.g. Field 1959). In the ISM, collisions of hydrogen atoms with other particles dominate. However, radiative effects will dominate closer to the AGN. Therefore, the spin temperature is considered to vary between a few hundred Kelvin to several thousand Kelvin. This has been confirmed by a few studies (Holt et al. 2006; Struve et al. 2010). Constraints on the spin temperature can be obtained from H I emission measurements, but these are only available for a very limited number of sources and the emitting H I is often on other spatial scales than the absorbing gas.

While the variety of radio telescopes in the EVN provides some challenges as stated above, it also results in unique capabilities. The EVN includes very large radio telescopes which significantly boost its sensitivity.

In addition, the incorporation of the *e*-MERLIN array in the United Kingdom yields very important short spacings to recover faint and diffuse extended radio continuum emission and extended absorption. Thereby, observation with the EVN in combination with *e*-MERLIN can cover a large range of angular scales from several arcsec to mas. This is particularly important for wide-field VLBI observations. Further strength of the EVN is the strong drive for technological developments and user support from setting up observations to processing the data. This ensures that the H I VLBI capabilities will continue to improve towards the SKA era and that the data are used efficiently.

2.2.5 Requirements and synergies

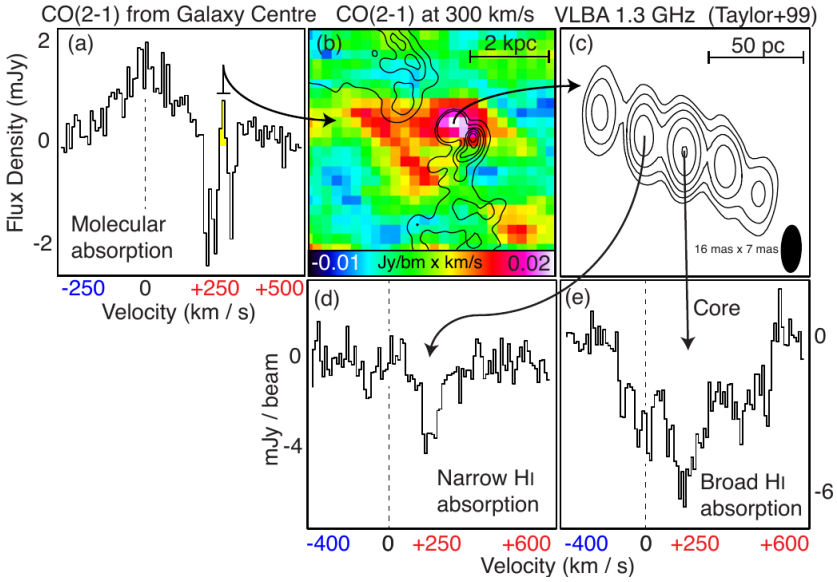

Figure 2.11: ALMA-detected CO(2-1) absorption and emission and VLBI-detected H I absorption show that the inflowing molecular gas clouds in Abell 2597 are likely to be located close to the central black hole (Tremblay et al. 2016).

Utilising the full capabilities of VLBI for H I absorption studies requires primarily an accurate calibration of the bandpass and good RFI mitigation. The latter is especially challenging for the short spacing provided by *e*-MERLIN which is essential to cover a large field of view and recover extended gas as well as continuum emission. In principle the resolution of VLBI is also sufficient to investigate the properties of H I gas over a larger redshift range. This will provide vital insight